Available online at www.sciencedirect.com

ScienceDirect

journal homepage: www.elsevier.com/locate/bbe

Original Research Article

Electroencephalography (EEG) signal processing for epilepsy and autism spectrum disorder diagnosis

Sutrisno Ibrahim, Ridha Djemal *, *Abdullah Alsuwailem*

Electrical Engineering Department, King Saud University, Riyadh, Saudi Arabia

ARTICLE INFO

Article history:
Received 11 June 2017
Received in revised form
24 August 2017
Accepted 29 August 2017
Available online 14 September 2017

Keywords:
EEG
Computer aided diagnosis
Epilepsy
Neurological disorder
Autism
Machine learning

ABSTRACT

Quantification of abnormality in brain signals may reveal brain conditions and pathologies. In this study, we investigate different electroencephalography (EEG) feature extraction and classification techniques to assist in the diagnosis of both epilepsy and autism spectrum disorder (ASD). First, the EEG signal is pre-processed to remove major artifacts before being decomposed into several EEG sub-bands using a discrete-wavelet-transform (DWT). Two nonlinear methods were studied, namely, Shannon entropy and largest Lyapunov exponent, which measure complexity and chaoticity in the EEG recording, in addition to the two conventional methods (namely, standard deviation and band power). We also study the use of a cross-correlation approach to measure synchronization between EEG channels, which may reveal abnormality in communication between brain regions. The extracted features are then classified using several classification methods. Different EEG datasets are used to verify the proposed design exploration techniques: the University of Bonn dataset, the MIT dataset, the King Abdulaziz University dataset, and our own EEG recordings (46 subjects). The combination of DWT, Shannon entropy, and k-nearest neighbor (KNN) techniques produces the most promising classification result, with an overall accuracy of up to 94.6% for the three-class (multi-channel) classification problem. The proposed method obtained better classification accuracy compared to the existing methods and tested using larger and more comprehensive EEG dataset.

The proposed method could potentially be used to assist epilepsy and ASD diagnosis therefore improving the speed and the accuracy.

1. Introduction

Computer-based systems have many applications in the medical field, such as for electronic health records (EHR) systems, hospital information systems (HISs), and computer-aided diagnosis (CAD) systems. Computer system can be used by medical doctors to diagnose certain disorders by automatically analyzing medical images [1] or physiological signals recorded from patients, such electroencephalography (EEG) signals [2]. Medical diagnosis is often a challenging task that requires deliberate effort and expertise from medical experts.

* *Corresponding author at*: Electrical Engineering Department, King Saud University, P.O. Box 800, 11421 Riyadh, Saudi Arabia.
E-mail addresses: suibrahim@ksu.edu.sa (S. Ibrahim), rdjemal@ksu.edu.sa (R. Djemal), suwailem@ksu.edu.sa (A. Alsuwailem).
http://dx.doi.org/10.1016/j.bbe.2017.08.006

With advances and developments in signal processing and machine learning methods, computer-based systems have become able to perform more sophisticated tasks, including EEG signal analysis. These automatic mechanisms would ultimately save time and improve global diagnosis accuracy.

Analyzing abnormality in brain signals may provide a clue to brain conditions and pathologies. EEG, which captures signals from the human brain, has great potential to be used for brain activity and condition analysis. EEG recordings have been used for a long time as a diagnostic tool for epilepsy [3]; recently, researchers have utilized EEG for autism spectrum disorder (ASD) diagnosis purposes [4]. Alzheimer's [5] and other neurological disorders are among targets of EEG-based analysis applications. Despite their low spatial resolution, EEG recordings have several advantages such as high temporal resolution, simplicity, lower costs, and wider availability.

In this paper, we investigate different feature extraction and EEG classification techniques for assisting epilepsy and autism spectrum disorder (ASD) diagnosis. After applying the pre-processing step, the discrete wavelet transform (DWT) and cross correlation approaches are used to extract features from the EEG signals. We combine DWT with several functions, including standard deviation (SD), band power (BP), Shannon entropy (SE), and largest Lyapunov exponent (LLE). We also compare different classification methods including artificial neural networks (ANNs), *k*-nearest neighbor (KNN), support vector machine (SVM), and linear discriminant analysis (LDA). The remainder of this paper is organized as follows. Section 2 describes the proposed methods, including feature extraction and classification techniques. Section 3 provides a description of the EEG data used during our experiments, the classification problem formulation, and the performance evaluation. Results and discussion are presented in Section 4. Section 5 provides our main conclusions and highlights of future research directions.

2. Methods

To build a CAD system for medical pathology diagnosis, we follow the four main steps depicted in Fig. 1, namely, acquisition of brain activities, pre-processing of EEG recordings, feature extraction, and classification. The acquired EEG signal is treated using a pre-processing block to remove any noise in brain patterns. An elliptic band-pass filter is used to efficiently limit the signals to a frequency between 0.5 and 60 Hz. We also investigated the different feature extraction and classification methods shown in the figure. We used the DWT and cross-correlation (measuring synchronization between EEG channels) to extract features from the EEG segment. For classification, we implemented ANN, KNN, SVM, and LDA.

Table 1 – Frequency bands for each wavelet coefficients.

Wavelet coefficients	Frequency (Hz)	EEG bands
D_3	32–64	Gamma
D_4	16–32	Beta
D_5	8–16	Alpha
D_6	4–8	Theta
A_6	0–4	Delta

DWT is able to capture small changes in the EEG signal by representing the signal in multi-scale time-frequency domains in terms of approximate (A_x) and detail (D_x) coefficients. In this work, we used six-level decomposition based on the Daubechies 4 (Db4) wavelet, which is commonly used for EEG analysis [6]. Only the D_3, D_4, D_5, D_6, and A_6 coefficients are used for feature extraction to represent the EEG sub-bands in the 0- to 32-Hz spectrum range. As shown in Table 1, these wavelet coefficients correspond to several EEG sub-bands, namely, delta (1–4 Hz), theta (4–8 Hz), alpha (8–15 Hz), beta (15–30 Hz), and gamma (30–60 Hz). More details regarding DWT and brain pattern rhythms are presented in [7]. Fig. 2 shows an example of the EEG signal and its DWT outputs (different labeled EEG sub-bands). EEG sub-bands with higher frequency, i.e., beta and gamma, have lower magnitude or power than lower frequency sub-bands, i.e., delta, theta and alpha.

We propose combining the discrete wavelet transform (DWT) with several statistical functions to build more efficient feature vectors. In fact, DWT can be associated with SD, BP, SE, and LLE. For a discrete time series of data $S[n]=[s_1\ s_2 \ldots s_N]$ with a length N, the standard deviation is calculated as follows:

$$SD = \sqrt{\frac{1}{N}\sum_{n=1}^{N}(s_n-\mu)^2} \quad (1)$$

where μ is the mean of the discrete data.

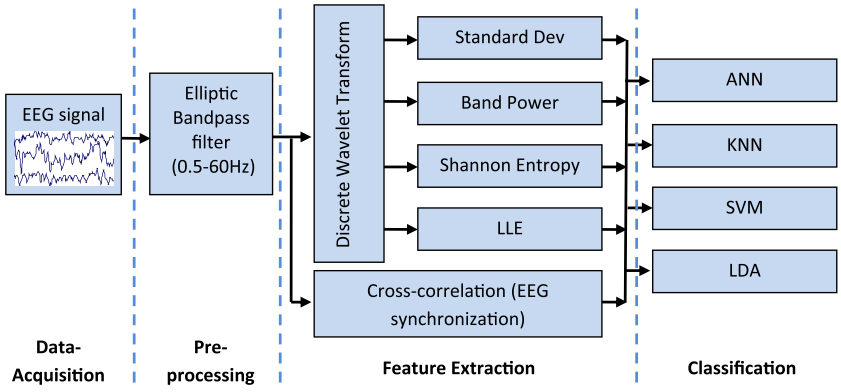

Fig. 1 – Generic block diagram of CAD system for medical pathology diagnosis.

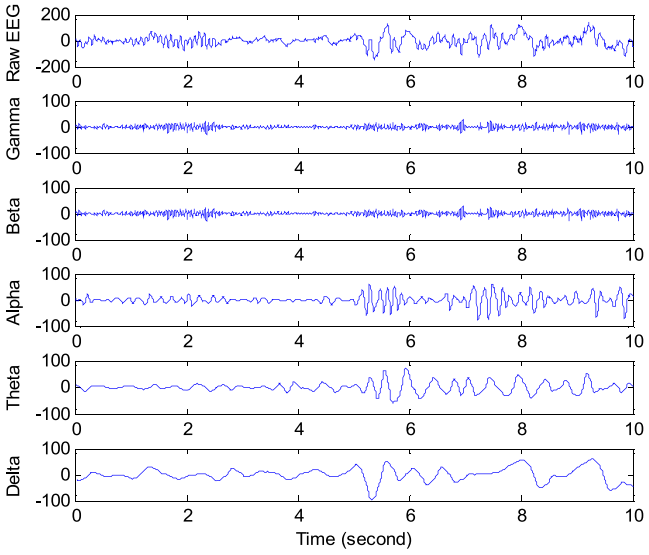

Fig. 2 – Raw EEG signal and its sub-bands extracted using DWT.

On the other hand, the BP of a signal is obtained by:

$$BP = \frac{1}{N}\sum_{n=1}^{N}(s_n)^2 \tag{2}$$

The SE [8] measures the distribution of the data in the EEG signal. SE can be calculated using the following formula:

$$SE = -\sum_{i=1}^{k} p_i \log_2 p_i \tag{3}$$

In which k is the number of unique values in the discrete data (S) and p_i is the probability or normalized frequency of the unique values. LLE quantifies the chaoticity of the signal. There are several algorithms to calculate LLE. In this study, we calculate LLE using Rosenstein's algorithm [9]. The first step in estimating the LLE is reconstructing the attractor dynamic from a single time series $[s_1\ s_2\ \ldots\ s_N]$. The reconstructed trajectories, $\mathbf{S}$, can be expressed as a matrix in which each row represents a phase-space vector. That is,

$$\mathbf{S} = \begin{bmatrix} S_1 & S_{1+p} & \cdots & S_{1+(m-1)p} \\ \vdots & \vdots & \vdots & \vdots \\ S_M & S_{M+p} & \cdots & S_{1+(m-1)p} \end{bmatrix} \tag{4}$$

Thus, $\mathbf{S}$ is an $M \times m$ matrix and all constants m, M, p, and N are linked by the following expression: $M = N - (m-1)p$, where m is the embedding dimension and p is the delay time (which should be chosen based on a given signal). The nearest neighbor, S_j, is found by searching the space point that minimizes the distance to a particular reference phase-space point, S_j which is expressed by:

$$d_j(0) = \min_{S_j} ||S_j - S_j|| \tag{5}$$

where $d_j(0)$ is the initial distance from the jth point to its nearest neighbor. The LLE is then estimated as the mean rate of separation between the nearest neighbors in the phase space vector, that is,

$$\lambda(i) = \frac{1}{i\Delta t}\frac{1}{(M-1)}\sum_{j=1}^{M-i}\ln\left(\frac{d_j(i)}{d_j(0)}\right) \tag{6}$$

where Δt represents the sampling period of the time series and $d_j(i)$ is the distance between the jth pair of nearest neighbors after i discrete time steps. Further details regarding the computation of the LLE can be found in [9]. The feature size for each single-channel EEG segment is fixed at 5, whereas for multi-channel EEG, it is fixed at 15 (5×3). In multi-channel EEGs, channels are grouped into three brain regions: anterior, central, and posterior, as shown in Fig. 3. The average value of the feature vector is calculated for each brain region.

Another method for feature extraction is based on EEG synchronization, which consists of three main steps: preprocessing and wavelet decomposition, measuring synchronization within and between brain regions, and classification. We study synchronization within and between different regions (frontal, central, and posterior) for each corresponding EEG sub-band (delta, theta, alpha, beta, and gamma). Abnormal connectivity and synchronization between brain regions may reveal certain brain disorders and pathologies, including epilepsy and ASD. In this study, we quantify synchronization between EEG channels using a cross-correlation function [10]. The cross-correlation between two signal x_n and y_n ($n = 1, 2, \ldots, N$) is calculated as:

$$C_{xy}(\tau) = \frac{1}{N-\tau}\sum_{i=1}^{N-\tau}\left(\frac{x_i - \hat{x}}{\sigma_x}\right)\left(\frac{y_i - \hat{y}}{\sigma_y}\right) \tag{7}$$

where $\hat{x}$ and σ_x denote the mean and the variance, respectively, and τ is the time lag. The absolute value of cross-correlation ranges from 0 (no synchronization) to 1 (maximum synchronization) and is symmetrical: $C_{xy}(\tau) = C_{yx}(\tau)$. By calculating the cross-correlations over all EEG channel pairs, we obtain the connectivity matrix. The size of this connectivity matrix depends on the number of channels. For example, for 16 EEG channels, the size of connectivity matrix is equal to 6×16. As done before, we grouped the EEG channels into three brain regions (anterior, central, and posterior). Then, we calculated

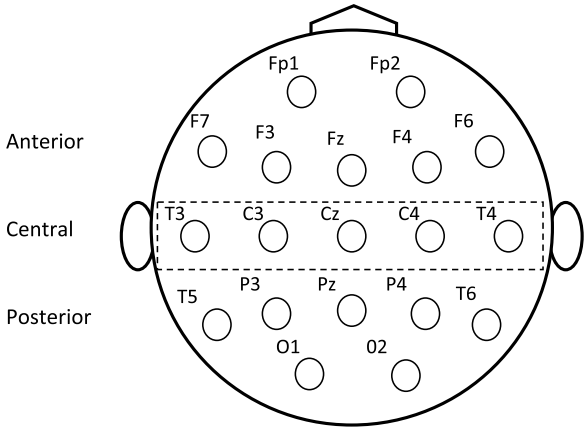

Fig. 3 – EEG channels grouped into three brain regions: anterior, central, and posterior.

the average EEG synchronization within and between all brain regions. For each EEG segment, we obtain six synchronization values in the form of a feature vector, which represents the synchronization, namely, within anterior, within central, within posterior, anterior-central, anterior-posterior, and central-posterior channels.

Regarding the classification techniques studied in this work, four different classifiers were used for EEG recording classification, namely, ANN, KNN, SVM, and LDA.

- The ANN technique:

  ANNs are widely used in the biomedical engineering field, such as in modeling, data analysis, diagnostics, and detection. In this work, we designed an ANN system with one input layer, one hidden layer, and one output layer. The hidden layer has five nodes and a log-sigmoid transfer function. The number of nodes in the input layer depends on the size of the input features, whereas the number of nodes in the output layer depends on the classification target (2 or 3 nodes). The output layer is designed with a soft-max (normalized exponential) transfer function.
- The KNN technique:

  KNN is among the simplest machine learning algorithms that classifies an object by a majority vote of its k-nearest neighbors [11]. In this work, k is equal to 3 for all experiments.
- The SVM and LDA techniques:

  Both SVM and LDA classification techniques use hyper-plane separation to classify their inputs. SVM is a supervised learning method that analyzes data and recognizes patterns, and is used for classification and regression analysis. Given a set of training examples, an SVM training algorithm builds a model (i.e., the separation hyper-plane) that assigns new examples into single categories [12]. In this study, we use a linear SVM instead of a non-linear SVM (such as that used in [13]); a non-linear SVM is expected to have higher computational costs and be slower to compute. In essence, the SVM is a binary (two-class) classifier. To address the three-class classification problem, in this study, we combine three SVM classifiers with a one-versus-all method. LDA is a generalization of Fisher's linear discriminant; it is based on mean vectors and covariance matrices of feature vectors for individual classes. LDA also uses a hyper-plane to differentiate between classes, reducing the variance within the class and exploiting the variance between the classes [14].

3. EEG data and classification problem formulation

3.1. *EEG data*

Different EEG datasets are used in this study to verify the proposed methods. The first dataset is provided by the University of Bonn, Germany. This dataset contains five sets, named A, B, C, D, and E, where each set includes exactly 100 single-channel EEG segments. Sets A and B were recorded using scalp EEGs from a normal person, whereas sets C, D, and E were recorded using intracranial EEGs from epileptic patients. The data were recorded with a sampling rate of 173.61 Hz. The total duration of each segment was approximately 23.6 s. A more detailed description of this dataset is provided in [15].

The second dataset was provided by a research team from MIT, USA [16]. The data contain 906 h of EEG data recorded from 23 epileptic patients. In this study, only data for the first ten subjects was used. This data includes 23 EEG channels; the sampling rate is 256 Hz [17]. The third dataset was provided by King Abdulaziz University (KAU), Saudi Arabia [18]. This dataset was recorded from ten normal subjects (males, aged 9–16 years) and nine autistic subjects (six male and three female, aged 10–16 years). The dataset was recorded in a relaxed state with 16-channel EEG at a sampling rate of 256 Hz.

We also record EEGs from ten normal subjects using our own setup using the g.tech software and hardware package [19]. The data acquisition setup includes a g.Gamma cap with 64 active EEG electrodes (g.Scarabeo), electrode drivers (terminal), multi-channel signal amplifier (g.Hiamp), and

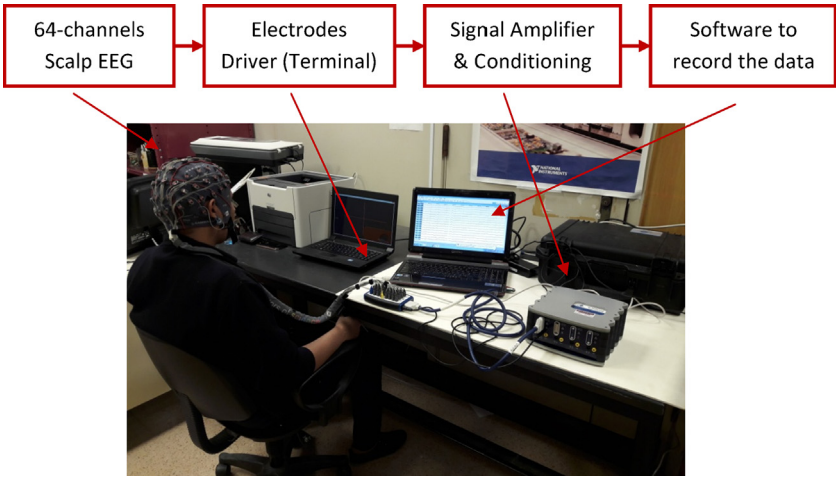

Fig. 4 – Our EEG data acquisition setup.

Table 2 – Classification problem formulations.

Category	Classification problem	EEG data
Two-class	Epileptic vs. normal (single-channel)	Set A vs. Set E from University of Bonn dataset. Total of 200 EEG segments (single-channel)
	Autistic vs. normal (single-channel)	King Abdulaziz University dataset. Total of 3040 EEG segments (single-channel)
	Autistic vs. normal (multi-channel)	King Abdulaziz University dataset. Total of 190 EEG segments (16-channel)
Three-class	Epileptic vs. autistic vs. normal (single-channel)	Total 3302 EEG segments (single-channel): University of Bonn (300 normal and 200 epileptic), KAU (480 normal and 432 autistic), MIT (690 epileptic), and our data (1200 normal)
	Epileptic vs. autistic vs. normal (multi-channel)	Total 390 EEG segments (multi-channel): KAU 16 channels (100 normal and 90 autistic), MIT 23 channels (100 epileptic), and our data 60 channels (100 normal)

software (g.Recorder) (as shown in Fig. 4). During the recording, all subjects were in a resting state with their eyes open. The data is recorded using a 64-channel EEG based on the 10–20 international standard acquisition system, with Fz as ground and the right ear as a reference. Only 60 channels were used in the current study. Data were recorded using a sampling rate of 256 Hz for a duration of at least 5 min for each subject. The recording was performed with all subjects' consent and permission.

3.2. *Classification problem formulations*

Diagnosis is a complex process, because it requires the experience of medical doctors or experts. However, we can reduce the diagnosis problem to a classification problem so as to simplify the problem formulation. The formulation of the classification problem depends on the analysis or diagnosis to be carried out. Five classification problems are addressed in this study, as summarized in Table 2.

There are three two-class classification problems: *epileptic vs. normal* (single-channel), *autistic vs. normal* (single-channel), and *autistic vs. normal* (multi-channel); and two three-class classification problems: *epileptic vs. autistic vs. normal* (single-channel) and *epileptic vs. autistic vs. normal* (multi-channel). The table also shows the EEG data used for each classification problem. All EEG segments have a duration of 23.6 s with a sampling rate of 256 Hz. As noted above, the University of Bonn dataset is up-sampled (from 173.61 to 256 Hz) to achieve a uniform sampling frequency.

3.3. *Performance evaluation*

In all of our experiments, 10-fold cross-validation is used as a validation technique. The data is randomly partitioned, into 10 subsets with the same size and with the same number of EEG segments. One subset is taken as the testing data, whereas the remainder is used as training data. As an example, in the first classification problem (*Epileptic vs. Normal*), 20 segments are used for training and the remaining 180 segments are used for testing. This process is repeated 10 times, such that every subset is used as testing data exactly once. The average accuracy of all experiments is used as the final performance metric.

4. Results and discussion

4.1. *Feature analysis*

Before performing EEG classification, we first analyze the EEG signals and the extracted features. Figs. 5–7 show EEG power spectral density and electrode maps for normal, autistic, and epileptic subjects, respectively. As noted above, the normal and autistic EEGs are taken from the KAU dataset, whereas the epileptic EEG is taken from the MIT dataset. The power spectral density is shown with a logarithmic scale to simplify the visualization. The electrode map is shown for the three different frequencies: 6 Hz (within the theta band), 10 Hz (alpha), and 22 Hz (beta). In general, the low frequency spectrum has higher power density than the high frequency spectrum. Frequencies above 30 Hz, i.e., the gamma band and above, have negligible power. Usually, this high frequency range can be treated as noise in the EEG. Comparing the three subjects, we see different power spectral density patterns. The subject with ASD has higher theta powers than the normal subject, which confirms the results of a previous study by Murias et al. [20].

To demonstrate the effectiveness of the extracted features for differentiating between the classes (or subjects), we

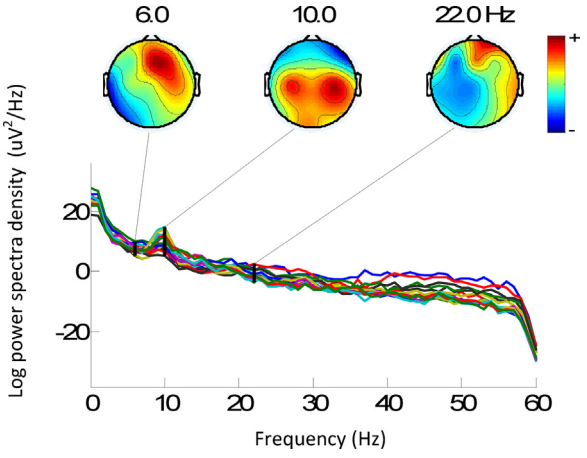

Fig. 5 – Power spectral density and electrode map for normal EEG.

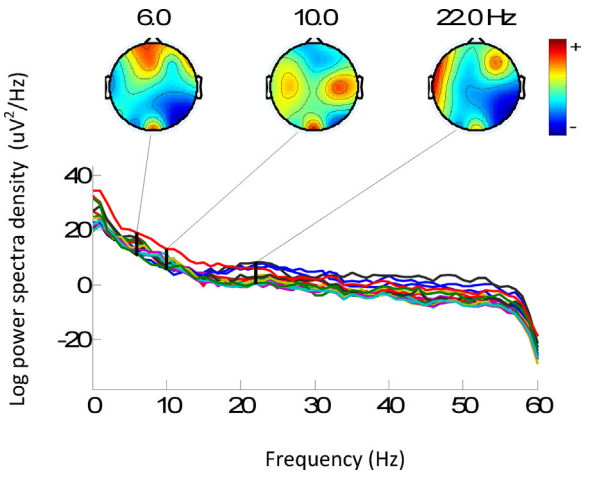

Fig. 6 – Power spectral density and electrode map for autistic EEG.

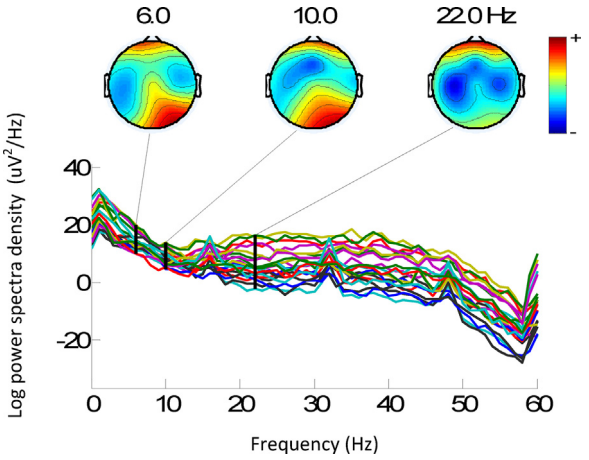

Fig. 7 – Power spectral density and electrode map for epileptic EEG.

visualize them in Cartesian coordinates. Figs. 8–11 show the features extracted using DWT combined with several functions, namely, SD, BP, SE, and LLE. The feature vector size for each single-channel EEG segment is equal to 5, which represents the extracted values within the EEG sub-bands, namely, delta, theta, alpha, beta, and gamma. SE shows the best ability to differentiate between the three types of EEG data, followed by SD. LLE shows the worst ability to differentiate between the subjects. As shown in Fig. 10, the epileptic EEG has higher SE values in almost all sub-bands, as compared with normal and autistic EEGs. Autistic EEGs also have higher SE values than normal EEGs. As mentioned above, SE measures the distribution of the data, in our case, representing the complexity of the EEG signals.

Fig. 12 shows EEG synchronization within and between brain regions calculated using the cross-correlation function. There are six synchronization values that forma feature vector: within anterior, within central, within posterior, anterior–central, anterior–posterior, and central–posterior channel synchronization. Compared with epileptic EEGs, autistic EEGs are more difficult to differentiate from normal EEGs, as shown in the figure.

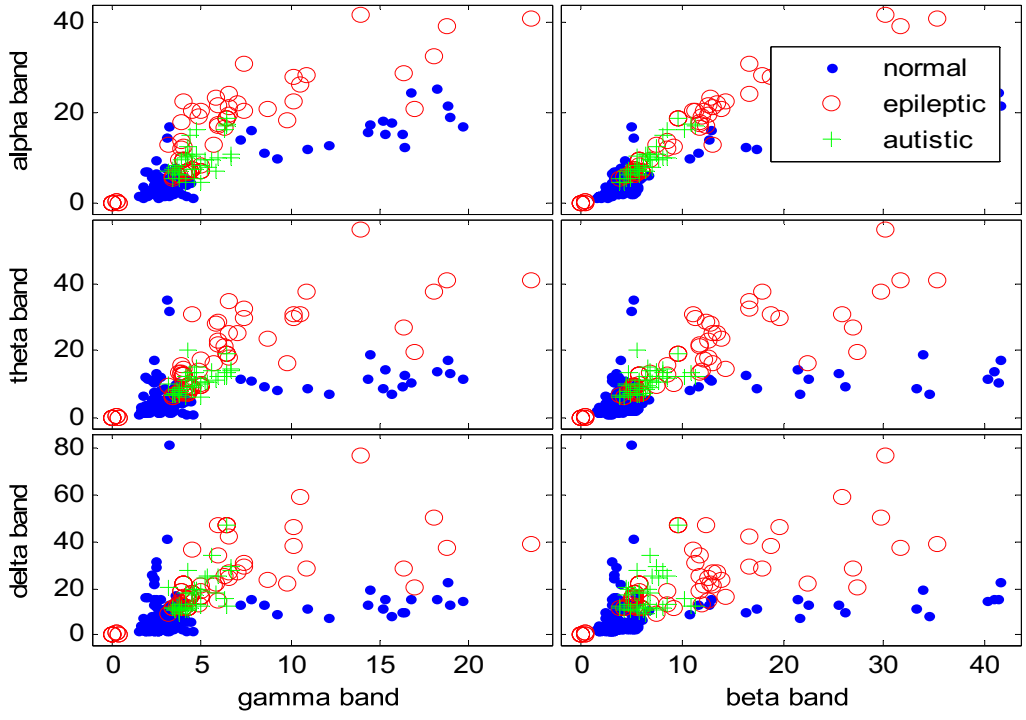

Fig. 8 – SD values within EEG sub-bands.

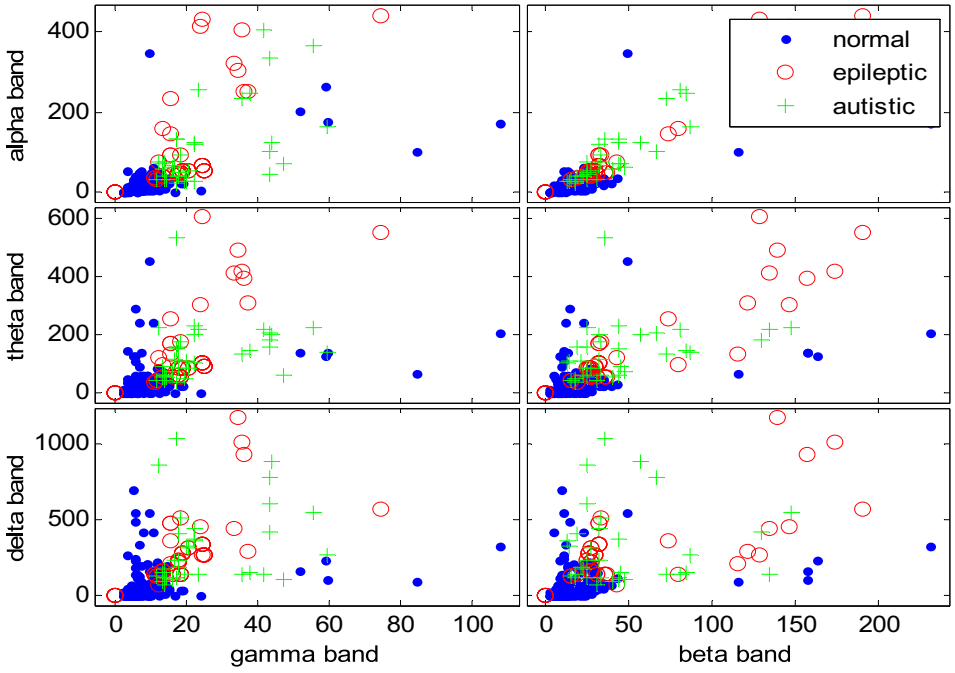

Fig. 9 – BP values within EEG sub-bands.

4.2. *Two-class (normal vs. epileptic) problem*

We start with the two-class classification problem that is classifying normal and epileptic EEG. As mentioned in Section 3.2, only the University of Bonn dataset is used for this classification problem, with a total of 200 EEG segments (from set A and set E). Table 3 shows a summary of the classification accuracy for different combinations of feature extraction methods and classification methods. Several possible combinations of feature extraction and classification methods achieve perfect performance (100%) in term of accuracy. Table 4 presents summary of EEG-based epilepsy diagnoses

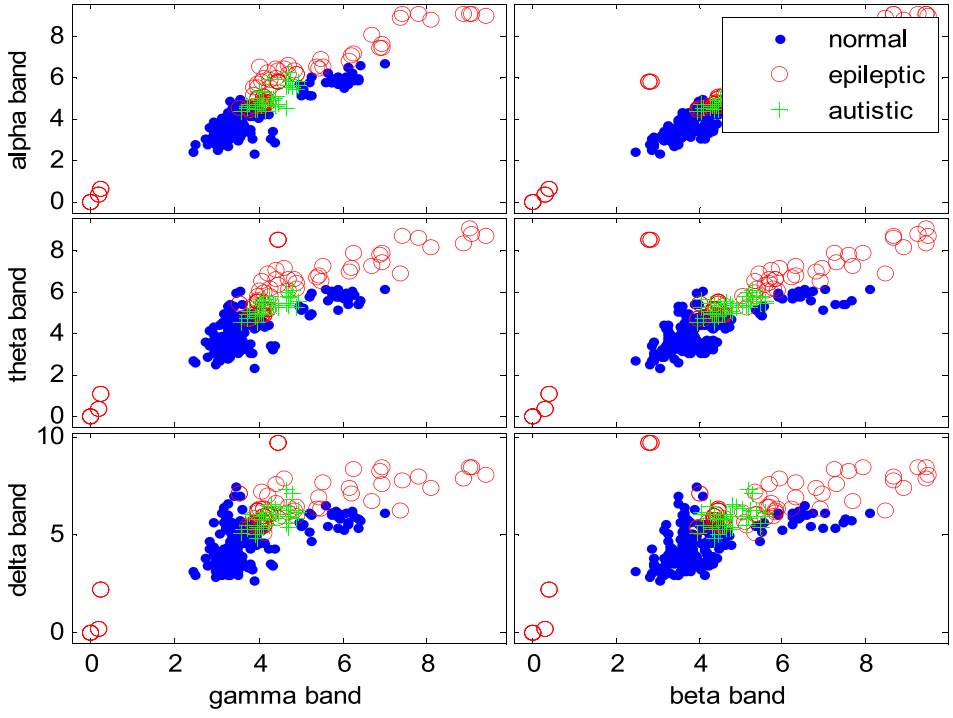

Fig. 10 – SE values within EEG sub-bands.

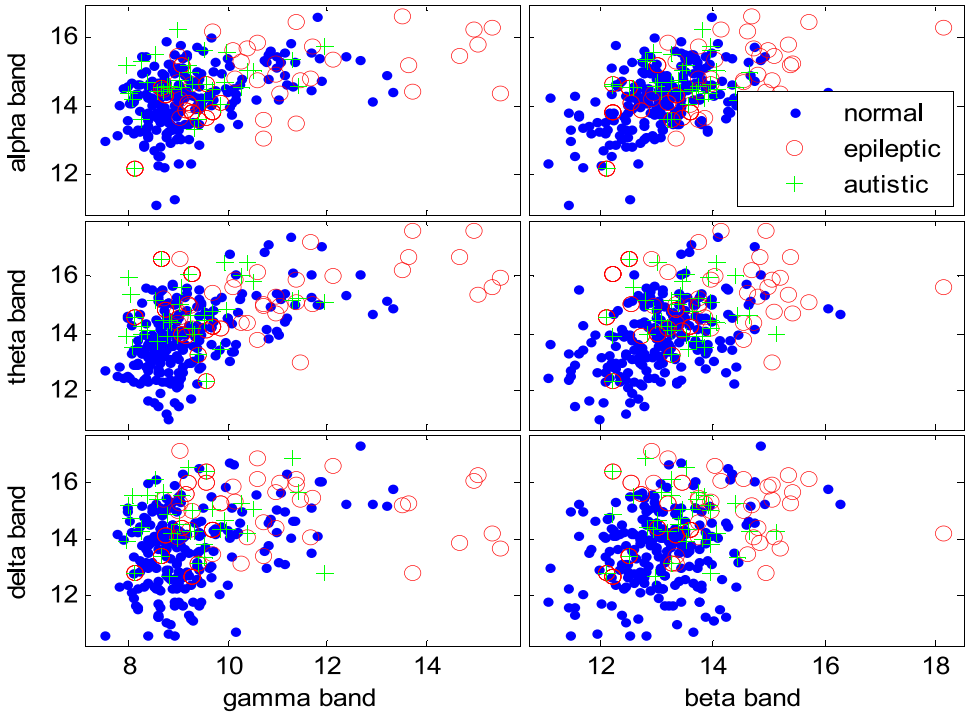

Fig. 11 – LLE values within EEG sub-bands.

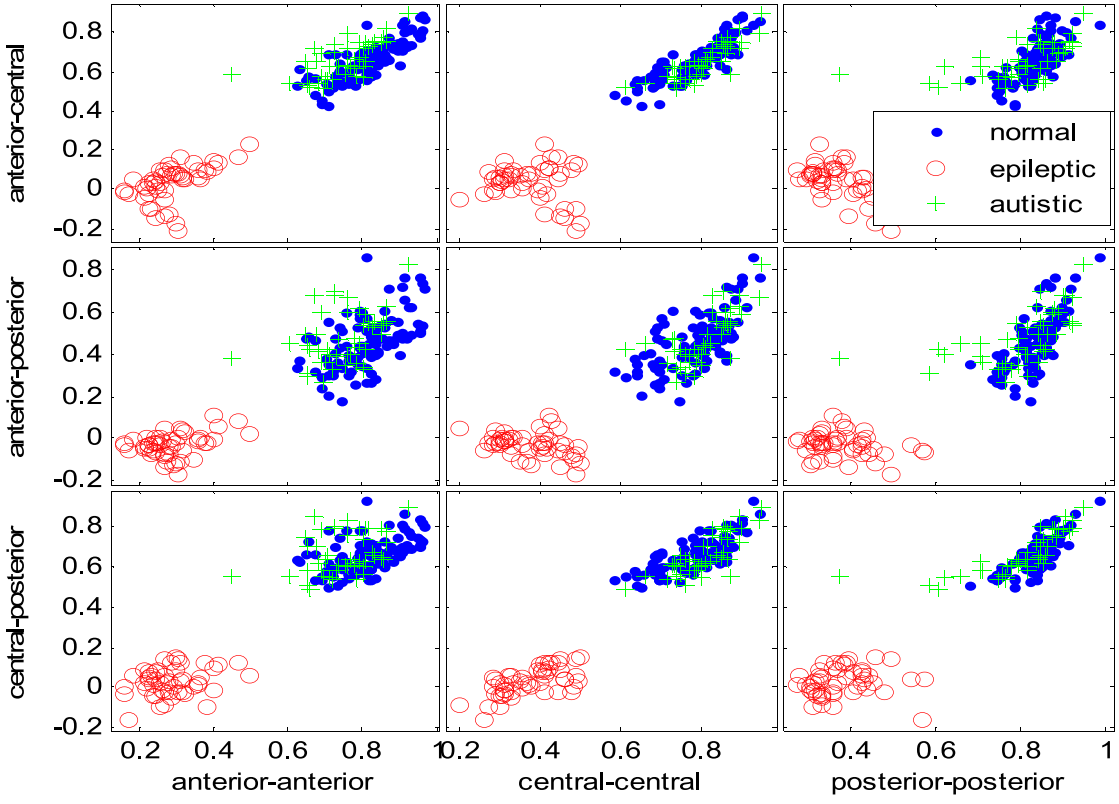

Fig. 12 – EEG synchronization within and between brain regions.

Table 3 – Classification accuracy for normal vs. epileptic EEG (single-channel).

Feature Extraction (feature size)	ANN (Acc %)	KNN (Acc %)	SVM (Acc %)	LDA (Acc %)
Wavelet+STD (5)	85	**100**	**100**	90
Wavelet+BP (5)	80.50	**100**	95.50	81.50
Wavelet+SE (5)	95	**100**	**100**	99
Wavelet+LLE (5)	77.50	90.50	92.50	90.50

Bold letter indicates the highest accuracy.

Table 4 – Comparison with several previous studies of epilepsy diagnosis.

Author	Feature extraction	Classifier	Acc (%)
Niqam et al., 2004 [21]	Non-linear filter	ANN	97.2
Kannathal et al., 2005 [22]	Entropies	ANFIS	92.2
Subasi et al., 2007 [23]	DWT	Mixture of expert (ME)	94.5
Srinivasan et al., 2007 [24]	Approximate entropy (Apen)	Elman ANN	100
Ocak 2009 [25]	Apen on DWT	ANN	96
Dhiman et al., 2014 [26]	DWT, GA-SVM	SVM	100
This work	DWT + SE/SD/BP	KNN/SVM	100

that used the same dataset (Bonn dataset, set A vs. set E). Several recent works have also achieved perfect classification performance. The Bonn dataset has been made publicly available for more than fifteen years; however, it is small and less comprehensive. It is necessary to validate the developed technique using larger and more comprehensive clinical databases.

4.3. *Two-class (normal vs. autistic) problem*

This section presents the results of the normal vs. autistic classification problem (single-channel and multi-channel EEG). Combinations of several datasets are used in this two-class classification problem (see Section 3.2 for more detail).

Table 5 – Classification accuracy normal vs. autistic EEG (single-channel).

Feature extraction (feature size)	ANN (Acc %)	KNN (Acc %)	SVM (Acc %)	LDA (Acc %)
Wavelet+STD 5)	8125	8355	7855	7385
Wavelet+BP (5)	8086	8118	7595	6961
Wavelet+SE (5)	8316	**8447**	7980	7954
Wavelet+LLE (5)	5938	5286	5885	5793

Bold letter indicates the highest accuracy.

Table 6 – Classification accuracy normal vs. autistic EEG (multi-channel).

Feature extraction (feature size)	ANN (Acc %)	KNN (Acc %)	SVM (Acc %)	LDA (Acc %)
Wavelet+STD (15)	8895	9053	9053	8316
Wavelet+BP (15)	7211	8421	8105	7368
Wavelet+SE (15)	9105	**9421**	9263	9368
Wavelet+LLE (15)	5842	6158	6263	6158
Cross-correlation (6)	8632	7895	8105	8263

Bold letter indicates the highest accuracy.

Table 5 shows the results for single-channel EEG data. Table 6 presents the multi-channel data. Note that cross-correlation is only applicable to multi-channel data. In general, multi-channel data leads to better accuracy than single-channel data. Overall, the combination of DWT+SE+KNN achieved the highest accuracy. Table 7 shows a comparison between our proposed method results and the existing methods for autism diagnosis. Note that the proposed method is validated using different datasets, which makes fair comparison for all methods difficult.

Table 7 – Several EEG-based autism spectrum disorder diagnosis methods.

Author	Feature extraction	Classifier	Dataset	Acc (%)
Bosl et al., 2011 [27]	Modified multiscale entropy (mMSE)	SVM	Own (USA)	70–100
Sheikhani et al., 2012 [28]	STFT, coherence	KNN	Own dataset	96.4
Ahmadlou et al., 2012 [29]	Wavelet, fuzzy SL	EPNN	Iranian dataset	95.5
Alhaddad et al., 2012 [18]	FFT	FLDA	Own (KSA dataset)	90
Our work	DWT, SE	ANN	Mixed	99.71

Table 8 – Classification accuracy normal vs. epileptic vs. autistic EEG (single-channel).

Feature extraction (feature size)	ANN (Acc %)	KNN (Acc %)	SVM (Acc %)	LDA (Acc %)
Wavelet+STD (5)	7328	9157	6486	4264
Wavelet+BP (5)	78.80	88.22	60.57	21.29
Wavelet+SE (5)	79.83	**92.94**	6414	60.81
Wavelet+LLE (5)	6829	7635	5697	5012

Bold letter indicates the highest accuracy.

Table 9 – Classification accuracy normal vs. epileptic vs. autistic EEG (multi-channel).

Feature extraction (feature size)	ANN (Acc %)	KNN (Acc %)	SVM (Acc %)	LDA (Acc %)
Wavelet+STD (15)	8641	9077	8590	8333
Wavelet+BP (15)	6231	8513	7923	7744
Wavelet+SE (15)	8795	**9462**	8615	8692
Wavelet+LLE (15)	6154	6256	6205	6128
Cross-correlation (6)	8718	8590	8282	8282

Bold letter indicates the highest accuracy.

4.4. *Three-class (normal vs. epileptic vs. autistic) problem*

Tables 8 and 9 show result summaries for the three-class classification problem, single-channel EEG, and multi-channel EEG, respectively. Use of different datasets, with different number of EEG channels and electrode positions, increases the problem complexity. Again, the combination of DWT+SE+KNN achieved the highest accuracy.

5. Conclusion and future directions

The ability to automatically analyze EEG data would improve the speed and accuracy of diagnosis processes. In this study, different EEG feature extraction and classification techniques for assisting epilepsy and autism spectrum disorder (ASD) diagnosis are presented. Different datasets are used to evaluate the proposed methods, with different numbers of EEG channels and electrode positions, which increases the problem complexity. The combination of DWT, SE, and KNN always achieved the best results, with an overall accuracy of 94.6% on the three-class classification problem (normal vs. epilepsy vs. autism). Future research directions include testing the proposed method with even larger datasets, and possibly with different levels of severity. Another neurological disorder such as Alzheimer's disease will be incorporated into the classification problem. Adaptive learning to improve the system performance over time will also be investigated.

Funding

This research was supported by a research project that is funded by King Abdulaziz City for Science and Technology (KACST), Saudi Arabia, Grant Number AT-34-147.

REFERENCES

[1] Doi K. Computer-aided diagnosis in medical imaging: historical review, current status and future potential. Comput Med Imaging Graph 2007;31(June–July (4–5)): 198–211.
[2] Acharya UR, Tree SV, Swapna G, Martis RJ, Suri JS. Automated EEG analysis of epilepsy: a review. Knowl Based Syst 2013;45:147–65.
[3] Noachtar S, Rémi J. The role of EEG in epilepsy: a critical review. Epilepsy Behav 2009;15(1):22–33.
[4] Bhat S, Acharya UR, Adeli H, Bairy GM, Adeli A. Automated diagnosis of autism: in search of a mathematical marker. Rev Neurosci 2014;25(6):851–61.
[5] Adeli H, Ghosh-Dastidar S, Dadmehr N. Alzheimer's disease: models of computation and analysis of EEGs. Clin EEG Neurosci 2005;36(3):131–40.
[6] Faust O, Acharya UR, Adeli H, Adeli A. Wavelet-based EEG processing for computer-aided seizure detection and epilepsy diagnosis. Seizure 2015;26(March):56–64.
[7] AlSharabi K, Ibrahim S, Djemal R, Alsuwailem A. A DWT-entropy-ANN based architecture for epilepsy diagnosis using EEG signals. 2016 2nd International Conference on Advanced Technologies for Signal and Image Processing (ATSIP); 2016. pp. 288–91.
[8] Shannon CE. A mathematical theory of communication. Bell Syst Tech J 1948;27(July–October (3)):379–423.
[9] Rosenstein MT, Collins JJ, De Luca CJ. A practical method for calculating largest Lyapunov exponents from small data sets. Phys D: Nonlinear Phenom 1993;65(May (1–2)):117–34.
[10] Quiroga RQ, Kraskov A, Kreuz T, Grassberger P. Performance of different synchronization measures in real data: a case study on electroencephalographic signals. Phys Rev E 2002;65:041903.
[11] Weinberger KQ, Saul LK. Distance metric learning for large margin nearest neighbor classification. J Mach Learn Res 2009;10(February):207–44.
[12] Burges CJC. A tutorial on support vector machines for pattern recognition. Data Min Knowl Discov 1998;2:121–67.
[13] Boser BE, Guyon IM, Vapnik VN. A training algorithm for optimal margin classifiers. Proceedings of the Fifth Annual Workshop on Computational Learning Theory – COLT'92; 1992. p. 144.
[14] Duda RO, Hart PE, Stork DG. Pattern classification; 2012.
[15] Andrzejak RG, Lehnertz K, Mormann F, Rieke C, David P, Elger CE. Indications of nonlinear deterministic and finite dimensional structures in time series of brain electrical activity: dependence on recording region and brain state. Phys Rev E 2001;64:061907.
[16] Goldberger A, et al. PhysioBank, PhysioToolkit, and PhysioNet: components of a new research resource for complex physiologic signals. Circulation 2000;101(23). e215–20. Link to database: http://physionet.org/pn6/chbmit/ [visited 05.09.16].
[17] Shoeb A. Application of machine learning to epileptic, seizure onset detection and treatment.[Ph.D. thesis] MIT; 2009.
[18] Alhaddad MJ, Kamel MI, Malibary HM, Alsaggaf EA, Thabit K, Dahlwi F, et al. Diagnosis autism by Fisher linear discriminant analysis FLDA via EEG. Int J Bio-Sci Bio-Technol 2012;4:45–54.
[19] g.BCIsys – g.tec's Brain-Computer Interface research environment. http://www.gtec.at/Products/Complete-Solutions/g.BCIsys-Specs-Features [visited 15.02.17].
[20] Murias M, Webb SJ, Greenson J, Dawson G. Resting state cortical connectivity reflected in EEG coherence in individuals with autism. Biol Psychiatry 2007;62(3):270–3.
[21] Nigam VP, Graupe D. A neural-network-based detection of epilepsy. Neurol Res 2004;26(6):55–60.
[22] Kannathal N, Lim CM, Acharya UR, Sadasivan PK. Entropies for detection of epilepsy in EEG. Comput Methods Programs Biomed 2005;80(3):187–94.
[23] Subasi A. EEG signal classification using wavelet feature extraction and a mixture of expert model. Expert Syst Appl 2007;32(4):1084–93.
[24] Srinivasan V, Eswaran C, Sriraam N. Approximate entropy-based epileptic EEG detection using artificial neural networks. IEEE Trans Inf Technol Biomed 2007;11(3):288–95.

[25] Ocak H. Automatic detection of epileptic seizures in EEG using discrete wavelet transform and approximate entropy. Expert Syst Appl 2009;36(2):2027–36.
[26] Dhiman R, Saini JS, Priyanka. Genetic algorithms tuned expert model for detection of epileptic seizures from EEG signatures. Appl Soft Comput 2014;19(June):8–17.
[27] Bosl W, Tierney A, Tager-Flusberg H, Nelson C. EEG complexity as a biomarker for autism spectrum disorder risk. BMC Med 2011;9(1):1–18.
[28] Ahmadlou H, Adeli H, Adeli A. Fuzzy synchronization likelihood-wavelet methodology for diagnosis of autism spectrum disorder. J Neurosci Methods 2012;211(2): 203–19.
[29] Sheikhani A, Behnam H, Mohammadi MR, Noroozian M, Mohammadi M. Detection of abnormalities for diagnosing of children with autism disorders using of quantitative electroencephalography analysis. J Med Syst 2012;36(April (2)):957–63.